Optics Letters

Multi-frequency phase-coded microwave signal generation based on polarization modulation and balanced detection

Dan Zhu, Weiyuan Xu, Zhengwu Wei, and Shilong Pan*

The Key Laboratory of Radar Imaging and Microwave Photonics, Ministry of Education, Nanjing University of Aeronautics and Astronautics, Nanjing 210016, China
**Corresponding author: pans@ieee.org*

Received 6 October 2015; revised 28 November 2015; accepted 2 December 2015; posted 2 December 2015 (Doc. ID 251490); published 21 December 2015

Photonic multi-frequency phase-coded microwave signal generation is proposed and demonstrated based on polarization modulation and balanced detection. Consisting of only a polarization modulator (PolM) driven by an electrical coding data, a polarization beam splitter (PBS) and a balanced photodetector (BPD), the proposed microwave phase coder has no requirement on the wavelength, intensity modulation format, or modulation index of the input optical microwave signal, and allows phase coding of arbitrary-format RF signals, which enables multi-frequency phase coding with compact structure, simple operation, and high flexibility. A proof-of-concept experiment is performed, achieving simultaneous phase coding of 15 and 30 GHz, or 10 and 20 GHz RF signals with a coding rate of 5 Gb/s.

OCIS codes: (060.5625) Radio frequency photonics; (070.1170) Analog optical signal processing; (280.5600) Radar.

http://dx.doi.org/10.1364/OL.41.000107

Phase-coded signal generation has attracted a lot of attention in the past decades, especially for radar applications, due to its pulse compression capability [1]. Conventionally, the phase-coded signal is generated in the electrical domain, which results in limited operational frequency range and a relatively small time-bandwidth product due to the inherent electronic bottleneck. To overcome these problems, photonic microwave phase-coded signal generation has been proposed and intensively studied, thanks to the high frequency, wide bandwidth, and immunity to electromagnetic interference enabled by the photonic technologies [2,3]. One method to generate the phase-coded signal is based on optical pulse shaping using a spatial light modulator (SLM) [4], but the system is bulky and lossy due to the use of free-space optics. Pure fiber optic schemes can efficiently solve these problems [5–10]. One such scheme is to heterodyne two phase-correlated optical wavelengths in which one wavelength is phase modulated [5–7], or to map two phase-correlated optical wavelengths into two orthogonal polarization directions followed by polarization modulation [8–10]. The key to the two approaches is how to separate the two wavelengths and get them phase modulated, respectively. The existing solutions are based on either optical filters or a length of polarization maintaining fiber, which inevitably limits the operational frequency range due to the wavelength-dependent operation.

On the other hand, the recent developments of multi-band and multifunctional radars [11] urgently demand simultaneous multi-frequency phase-coded signal generation, which is hard to implement using the approaches with wavelength-dependent devices. Although photonic microwave phase-coded signal generation without the use of wavelength-dependent components has been realized based on a phase modulator (PM) [12], a dual-parallel Mach–Zehnder modulator (DPMZM) [13], a dual-drive Mach–Zehnder modulator (DDMZM) [14], a dual-parallel PolM [15], a polarization modulator (PolM), together with a PM [16] or cascaded PolMs [17], few of them can implement simultaneous multi-frequency phase coding. For the photonic microwave phase coders based on single modulator [12–15], the introduction of multiple frequencies with the required power level would inherently generate many undesirable mixing components due to the nonlinearity of the electro-optic modulators, while for the approaches in [16] and [17], to implement multi-frequency phase coding, one separated PolM is required for each RF signal, and the magnitude of the RF signal should be equal to the half-wave voltage of the PolM at the frequency of the RF signal, or precise polarization alignment is required. Recently, Ghelfi *et al.* proposed an approach to generate phase-coded RF signals at multiple frequencies by upconverting an electrical phase-coded signal at intermediate frequency (IF) to the RF band based on intensity modulation of ultrashort pulses from a mode-locked laser (MLL) [18]. However, the phase coding is implemented in the electronic domain.

In this Letter, we propose and demonstrate a novel photonic microwave phase coder with simultaneous multi-frequency phase coding capability, consisting of a PolM driven by electrical coding data, a polarization beam splitter (PBS), and a balanced photodetector (BPD). As compared to the previous reported

photonic microwave phase coding schemes, the proposed photonic microwave phase coder can accept optical input signals carrying RF frequencies at any wavelengths, with arbitrary intensity modulation formats (double sideband modulation, single sideband modulation, carrier-suppressed double sideband modulation, etc.) and with arbitrary modulation indices. It also allows phase coding of arbitrary-format RF signals (single frequency signal, linear frequency modulated signal, etc.) by using an optical signal carrying RF signals with these formats. Thus, the proposed scheme enables multi-frequency phase coding with compact structure, simple operation, and high flexibility. In addition, the proposed system can output RF signals with frequencies that are higher than the maximal frequency of the electro-optic modulators if a photonic microwave multiplying technique is applied before the photonic microwave phase coder. A proof-of-concept experiment is carried out. An optical frequency comb (OFC) with three comb lines is employed to emulate the optical signal carrying multiple RF frequencies. Phased-coded signals at simultaneous 15 and 30 GHz and simultaneous 10 and 20 GHz with a coding rate of 5 Gbit/s are generated.

Figure 1 shows the schematic diagram of the proposed multi-frequency phase-coded signal generator based on polarization modulation and balanced detection. An optical signal with an optical field of $E_0(t)$ is injected into a PolM through a polarization controller (PC). By tuning the PC, the polarization state of the injected light is adjusted to have an angle of 45° to one principal axis of the PolM. An electrical coding data represented by $\phi(t)$ is introduced to drive the PolM. The output of the PolM can be expressed as

$$\begin{bmatrix} E_x \\ E_y \end{bmatrix} = \frac{\sqrt{2}}{2}\begin{bmatrix} E_0(t)\cdot\exp[j(\gamma\phi(t)+\varphi)] \\ E_0(t)\cdot\exp[-j\gamma\phi(t)] \end{bmatrix}, \tag{1}$$

where γ is the phase modulation index and φ is the phase difference between E_x and E_y, which can be tuned by adjusting the bias voltage of the PolM.

The output of the PolM is introduced to a PBS, of which the polarization axes have angles of α and $(\alpha+\pi/2)$ to one principal axis of the PolM. The optical fields of the two outputs of the PBS are given by

$$E_{\text{out1}} = E_x\cdot\cos\alpha + E_y\cdot\sin\alpha, \tag{2}$$

$$E_{\text{out2}} = E_x\cdot\cos(\alpha+\pi/2) + E_y\cdot\sin(\alpha+\pi/2). \tag{3}$$

Leading the two signals to a BPD and adjusting the bias voltage of the PolM to let $\varphi=\pi/2$, the RF current at the output of the BPD is written as

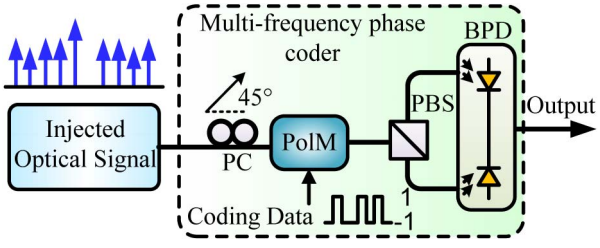

Fig. 1. Schematic of the proposed photonic multi-frequency phase-coded microwave signal generator based on polarization modulation and balanced detection. LD, laser diode; PC, polarization controller; PolM, polarization modulator; PBS, polarization beam splitter; BPD, balanced photodetector.

$$\begin{aligned} I(t) &= E_{\text{out1}}\cdot E_{\text{out1}}^{*} - E_{\text{out2}}\cdot E_{\text{out2}}^{*} \\ &= -|E_0(t)|^2\cdot\sin(2\alpha)\cdot\sin[2\gamma\phi(t)]. \end{aligned} \tag{4}$$

When $\phi(t)$ is '1' or '−1', we have

$$\sin[2\gamma\phi(t)] = \phi(t)\sin(2\gamma). \tag{5}$$

Thus, the result in Eq. (4) can be rewritten as

$$I(t) = -\phi(t)\cdot|E_0(t)|^2\cdot\sin(2\alpha)\cdot\sin(2\gamma). \tag{6}$$

As can be seen, bi-phase coding (either "0" or "π") of the RF signal carried in $E_0(t)$ is realized. The coding phase is only determined by the polarity of the electrical coding signal, with no connection to its magnitude. Since the phase coding is actually independent of $E_0(t)$, thus the wavelength, intensity modulation format (double sideband modulation, single sideband modulation, carrier-suppressed double sideband modulation, etc.), or modulation index will not affect the performance of the proposed photonic microwave phase coder. The modulation index γ will only affect the output power of the phase coding signal. If the optical signal $E_0(t)$ injected into the proposed photonic microwave phase coder carries multiple RF signals, simultaneous multi-frequency phase coding can be realized with compact structure, simple operation, and high flexibility. Phase coding of arbitrary-format RF signals can also be realized if $E_0(t)$ carriers arbitrary-format RF signals. In addition, it can be seen that the same coding phase is applied to the RF signals carried by $E_0(t)$. As an example, we consider a case when an OFC with a comb line angular spacing of ω_m is served as $E_0(t)$, i.e.,

$$\begin{aligned} E_0(t) = E_0\{&\exp(j\omega_0 t) + \exp[j(\omega_0+\omega_m)t] + \ldots \\ &+ \exp[j(\omega_0+(n-1)\cdot\omega_m)t]\}, \end{aligned} \tag{7}$$

where ω_0 is the angular frequency of the first line of the OFC, and n is the number of the comb lines. Then, we can get

$$|E_0(t)|^2 = E_0^2\cdot\left\{n+\sum_{k=1}^{n-1}2(n-k)\cos(k\omega_m t)\right\}. \tag{8}$$

Thus, the output RF current is written as

$$\begin{aligned} I(t) = -\phi(t)\cdot E_0^2\cdot&\left\{\sum_{k=1}^{n-1}2(n-k)\cos(k\omega_m t)\right\} \\ &\cdot\sin(2\alpha)\cdot\sin(2\gamma). \end{aligned} \tag{9}$$

From Eq. (9), we can see that binary phase coding of RF signals at multiple frequencies of $k\cdot\omega_m$ $(1\le k\le n-1)$ is implemented. Similar results can be obtained if the OFC is replaced by an ultrashort pulse from an MLL or a wavelength division multiplexing (WDM) signal carrying multiple RF frequencies.

A proof-of-concept experiment based on the setup shown in Fig. 1 is carried out. The injected OFC with three combs is generated by modulating a lightwave at 1550.11 nm from a laser diode (LD, Teraxion NLL04) at a Mach–Zehnder modulator (MZM, Fujitsu, FTM7938EZ). The bandwidth of the MZM is 40 GHz and the half-wave voltage is 2.8 V. The microwave signal introduced to the MZM is generated by a microwave signal generator (Agilent 8267D). The PolM (Versawave Technologies) has a bandwidth of 40 GHz and a half-wave voltage of 3.5 V. A pulse pattern generator (PPG, Anritsu MP1763C) is used to generate the electrical coding signal. The BPD (u^2t photonics, BPDV2150R) has a bandwidth of

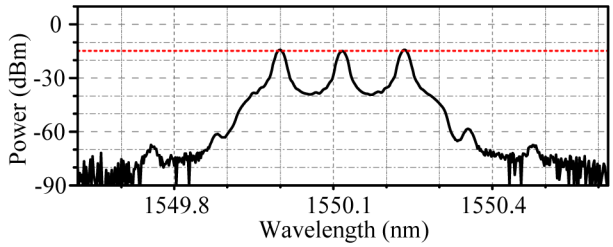

Fig. 2. Optical spectrum of the optical frequency comb with three comb lines at the output of the MZM.

40 GHz and a responsivity of 0.53 A/W. An optical spectrum analyzer (Yokogawa AQ 6370C) with a resolution of 0.02 nm is used to measure the optical spectra, and a digital storage oscilloscope (Agilent DSO-X92504A) with an instantaneous bandwidth of 32 GHz and a sampling rate of 80 GSa/s is employed to observe the waveforms.

To verify the simultaneous multi-frequency phase coding capability of the proposed scheme, an OFC with three comb lines is used as the injected light. Figure 2 shows the optical spectrum at the output of the MZM when the MZM is driven by a 4-dBm 15-GHz RF signal and biased at 2.4 V. The polarization direction of the OFC is adjusted to have an angle of 45° to one principal axis of the PolM by tuning PC1. A 5 Gbit/s electrical coding signal with a pattern of "1111-111-1 1-1-11 1-11-1" generated by the PPG is introduced to the PolM. The peak-to-peak voltage of the electrical coding signal is set to be 1.2 V. The generated signals at 15 and 30 GHz are selected by using a digital bandpass filter with a passband of 10 GHz centered at 15 and 30 GHz, respectively. Figure 3 shows the simultaneously generated phase-coded waveforms and the corresponding recovered phase profiles at 15 and 30 GHz. The duration of the generated signal corresponding to one integral pattern of "1111-111-1 1-1-11 1-11-1" is 3.2 ns. As can be seen, simultaneous phase coding at 15 and 30 GHz is realized. The recovered phase is 0° or 180°, corresponding to "1" or "-1" in the electronic coding signal, which is consistent with the theoretical analyses.

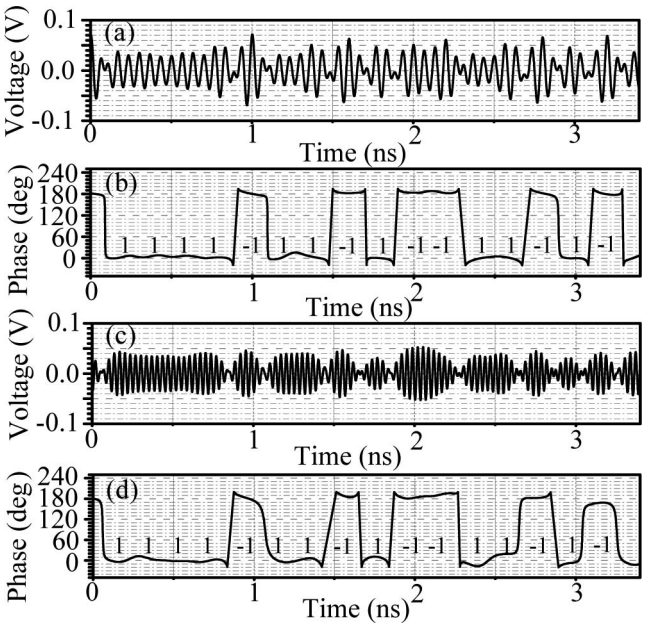

Fig. 3. (a) Waveform of the generated 15-GHz phase-coded signal and (b) the recovered phase profile. (c) Waveform of the generated 30-GHz phase-coded signal and (d) the recovered phase profile. The data rate and magnitude of the electrical coding signal are 5 Gbit/s and 1.2 V, respectively.

By increasing the peak-to-peak voltage of the electrical coding signal to 1.8 V, the waveforms of the generated phase-coded signals at 15 and 30 GHz and the corresponding recovered phase profiles are shown in Figs. 4(a)–4(d), respectively. By comparing the results with those in Fig. 3, we can find that the recovered phase profiles are not affected by the amplitude of the electrical coding signal, which agrees well with the theoretical analyses in Eq. (9). The pulse compression capability is also investigated with the autocorrelation results of the 15- and

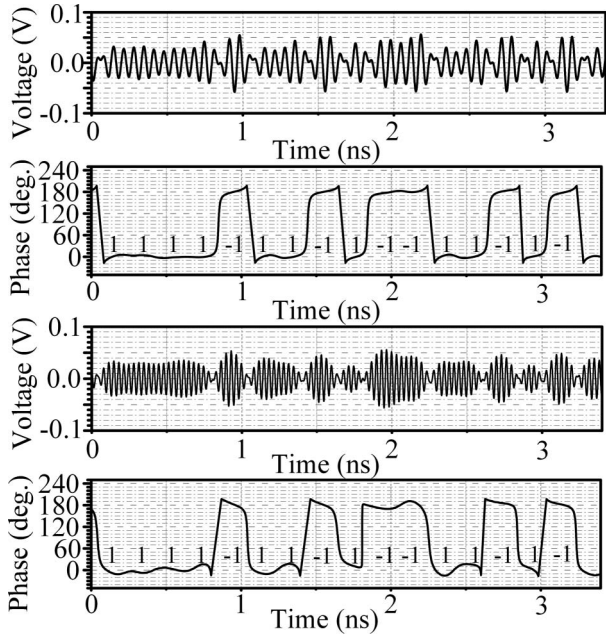

Fig. 4. (a) Waveform of the generated 15-GHz phase-coded signal and (b) the recovered phase profile. (c) Waveform of the generated 30-GHz phase-coded signal and (d) the recovered phase profile. The data rate and magnitude of the electrical coding signal are 5 Gbit/s and 1.8 V, respectively.

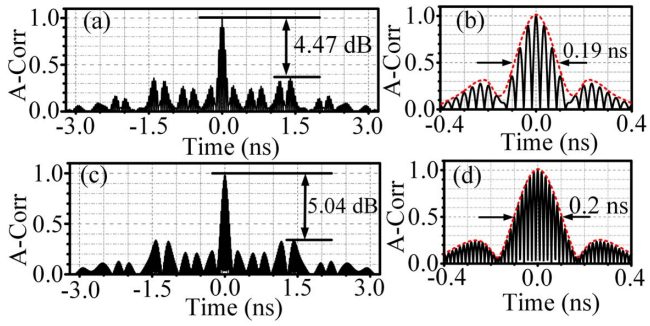

Fig. 5. (a) Autocorrelation of the generated 15-GHz phase-coded signal and (b) the zoom-in view of the main lobe. (c) Autocorrelation of the generated 30-GHz phase-coded signal and (b) the zoom-in view of the main lobe.

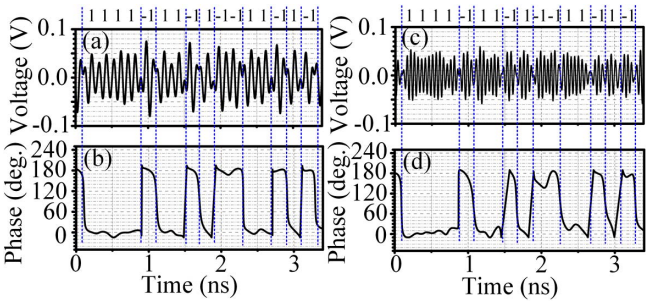

Fig. 6. (a) Waveform of the generated 10-GHz phase-coded signal and (b) the recovered phase profile. (c) Waveform of the generated 20-GHz phase-coded signal and (d) the recovered phase profile. The data rate and magnitude of the electrical coding signal are 5 Gbit/s and 1.8 V, respectively.

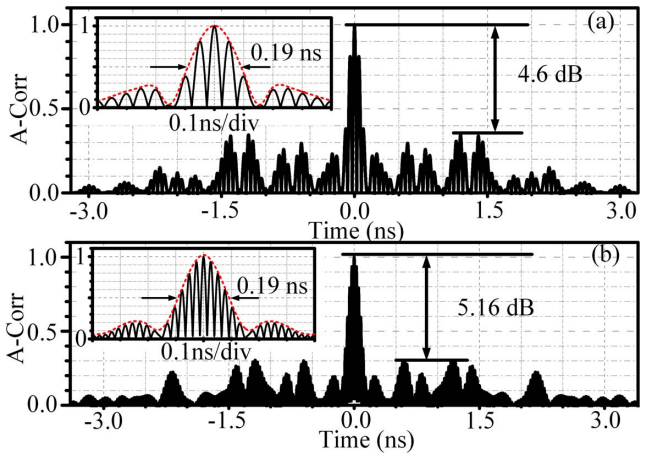

Fig. 7. (a) Autocorrelation of the generated 10 GHz phase-coded signal and (b) the zoom-in view of the main lobe. (c) Autocorrelation of the generated 20 GHz phase-coded signal and (b) the zoom-in view of the main lobe.

30-GHz phased-coded signals shown in Fig. 5. As can be seen, for the 15- and 30-GHz phase-coded signals, the peak-to-side-lobe ratios (PSRs) are about 4.47 and 5.04 dB, respectively. The full width at half-maximum (FWHM) of the main lobe is about 0.19 ns for the 15-GHz signal and 0.2 ns for the 30-GHz signal, giving a compression ratio of about 16.

Since no wavelength-dependent component is used, good frequency tunability can be achieved by simply adjusting the frequency of the RF signal in the OFC generator. For instance, when the spacing of the OFC is set to 10 GHz, phase-coded signals at 10 and 20 GHz are simultaneously generated, as shown in Fig. 6. The autocorrelation curves of the generated signals are shown in Fig. 7; they give a PSR of 4.6 dB, a main lobe FWHM of 0.19 ns, and a compression ratio of about 16 for the 10-GHz phase-coded signal; and a PSR of 5.16 dB, a main lobe FWHM of 0.19 ns, and a compression ratio of about 16 for the 20-GHz phase-coded signal.

In conclusion, we proposed and demonstrated a novel photonic microwave phase-coded signal generator with simultaneous multi-frequency phase coding capability based on polarization modulation and balanced detection. The proposed photonic microwave phase coder has no requirement on the wavelength, intensity modulation format, and modulation index of the input optical microwave signal, which provides multi-frequency phase coding capability with compact structure, simple operation, and high flexibility, and allows phase coding with arbitrary-format RF signals. Phase-coded signals at 15 and 30 GHz, or 10 and 20 GHz with a coding rate of 5 Gbit/s were experimentally generated by employing an OFC with three comb lines as the input optical signal. A phased-coded signal with more carrier frequencies can be realized by using an optical signal with more frequency components, such as an OFC with more comb lines, an ultra-short pulse from an MLL, and a single-wavelength or WDM signal carrying multiple RF frequencies. Phase coding of arbitrary-format RF signal can also be realized by using an optical signal carrying RF signals with these formats. The proposed scheme will bring the benefits of extended working frequency range and large working bandwidth for multi-frequency radars. This approach can find applications in multi-band and multifunctional radars.

Funding. National Basic Research Program of China (2012CB315705); National Natural Science Foundation of China (NSFC) (61201048, 61422108, 61527820); Aviation Science Foundation of China (2013ZC52040, 2013ZC52050); Fundamental Research Funds for the Central Universities (NJ20140006).

REFERENCES

1. M. I. Skolnic, *Introduction to Radar* (McGraw-Hill, 2001).
2. P. Ghelfi, F. Laghezza, F. Scotti, G. Serafino, A. Capria, S. Pinna, D. Onori, C. Porzi, M. Scaffardi, and A. Malacarne, Nature **507**, 341 (2014).
3. S. L. Pan, D. Zhu, and F. Z. Zhang, Trans. Nanjing Univ. Aeronaut. Astronaut. **31**, 219 (2014).
4. J. McKinney, D. Leaird, and A. Weiner, Opt. Lett. **27**, 1345 (2002).
5. Z. Li, W. Li, H. Chi, X. Zhang, and J. Yao, IEEE Photon. Technol Lett. **23**, 712 (2011).
6. H.-Y. Jiang, L.-S. Yan, J. Ye, W. Pan, B. Luo, and X. Zou, Opt. Lett. **38**, 1361 (2013).
7. P. Ghelfi, F. Scotti, F. Laghezza, and A. Bogoni, J. Lightwave Technol. **30**, 1638 (2012).
8. Z. Li, M. Li, H. Chi, X. Zhang, and J. Yao, IEEE Microw. Wirel. Compon. Lett. **21**, 694 (2011).
9. H. Chi and J. Yao, IEEE Microw. Wirel. Compon. Lett. **18**, 371 (2008).
10. Y. M. Zhang and S. L. Pan, Opt. Lett. **38**, 766 (2013).
11. G. C. Tavik, C. L. Hilterbrick, J. B. Evins, J. J. Alter, J. G. Crnkovich, Jr., J. W. de Graaf, W. Habicht, G. P. Hrin, S. Lessin, and D. C. Wu, IEEE Trans. Microwave Theory Tech. **53**, 1009 (2005).
12. W. Li, L. X. Wang, M. Li, and N. H. Zhu, IEEE Photon. Technol. Lett. **25**, 1867 (2013).
13. W. Li, L. X. Wang, M. Li, H. Wang, and N. H. Zhu, IEEE Photon. J. **5**, 5501507 (2013).
14. Z. Z. Tang, T. T. Zhang, F. Z. Zhang, and S. L. Pan, Opt. Lett. **38**, 5365 (2013).
15. S. F. Liu, D. Zhu, Z. W. Wei, and S. L. Pan, Opt. Lett. **39**, 3958 (2014).
16. W. Li, L. X. Wang, M. Li, and N. H. Zhu, Opt. Lett. **38**, 3441 (2013).
17. L. Gao, X. Chen, and J. Yao, IEEE Photon. Technol. Lett. **25**, 899 (2013).
18. P. Ghelfi, F. Scotti, F. Laghezza, and A. Bogoni, IEEE J. Quantum Electron. **48**, 1151 (2012).